



Morphological classification of M85, NGC 4394, NGC2336, NGC2841

Francesca Bazerla¹, Andrea Cristofoli², Enrico Delibori³, Damiano Fraizzoli¹, Alessandro Susca¹

¹Liceo G. Fracastoro, Verona

²Liceo E. Medi, Villafranca

³Liceo P. Levi, San Pietro in Cariano

Abstract. We obtained the morphological classification of four galaxies, M 85, NGC 2336, NGC 2841 and NGC 4394, studying isophotes parameters, comparing the brightness profile with empirical laws, de Vaucoulers' profile for the bulge and the exponential law for the disk and making a model of the brightness distribution using the isophotes approximated by ellipses. The observations were performed by 67/92 Schmidt Telescope, Asiago Observatory, in R band filter. The results obtained show a reasonable agreement to the literature.

1. Introduction

Galaxies are morphologically classified by Hubble's sequence in ellipticals, lenticulars, spirals and irregulars (Figure 1). Elliptical galaxies have regular disposition of stars, and appear as ellipses. They are denoted by the letter E, followed by a number from 1 to 7 representing their apparent ellipticity. Lenticulars are denoted by S0. Spirals have a central concentration of stars, called bulge, and a flattened disk, with star disposed in a spiral structure. They are divided in spirals and barred spirals, which have a bar-like structure near the bulge. They are denoted by letter S (spiral) or SB (barred spiral) followed by "a", "b", or "c" (Sa is a spiral with tightly-wound arms and with a bright central bulge; Sc has less wounded spiral arms and a weak bulge).

Our work was aimed to classify the observed galaxies in three ways: a) using the isophotes, approximated by ellipses, b) creating a model to subtract from the original images and analysing the residual image, c) analysing their brightness profile.

Isophotes are defined as lines that link points with the same brightness. Once the isophote are approximated by ellipses it is possible to analyse their ellipticity, polar angle and the coordinate of the centers as a function of the semi-major axis, these functions give informations about the morphology of the galaxies.

The second method is based on the modelization of the galaxy brightness, assuming the isophote like ellipses, now with fixed center. By the difference between the original image and the model, residual image, it is possible to infer the morphology.

Finally we can classify galaxies by calculating their T-Type, a number obtained by the difference between

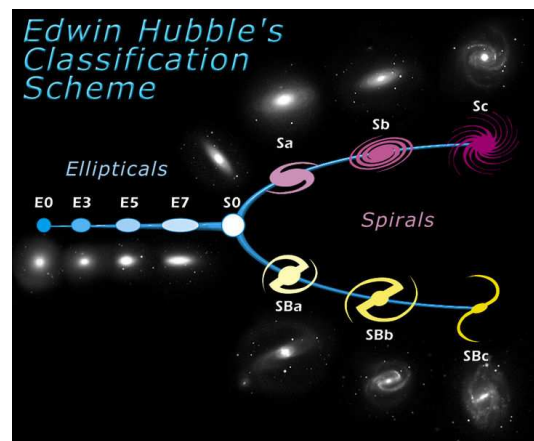


Fig. 1. Hubble's classification. (wikipedia)

Table 1. T-Type & Hubble's classification

T Type	Hubble
-5	E
-2	S0
+1	Sa
+3	Sb
+5	Sc

bulge and disk brightness. T-Type is related to a class of galaxy according to De Vaucouleurs and Simien classification (Table 1).

2. Observational data

The data we used has been taken by the 67/92 Schmidt Telescope, Asiago Observatory. The telescope is equipped with a CCD system, SBIG STL-11000M, detector KAI-11000M with 4008 x 2672 active pixels. The pixel has a surface of 9 microns square and the scale factor is 0,86 arcsec/pixel. The images were taken using R band filter (Figure 2). In Table 2 are shown the observational data.

The images have been corrected by dark, the constant response exhibited by CCD during periods when it is not actively being exposed to light, and flat field, in order to correct the different pixel response and the possible non-uniform illuminance of CCD.

Table 2. Galaxies and observational data

Galaxy	NGC2336	NGC2841	NGC4394	M85
Date	06/02/11	06/02/11	06/02/11	06/02/11
Hour	19:18:17	19:11:51	22:00:36	22:00:36
Exp time	600	300	300	300
RA	07h 26m 58s	09h 22m 08s	12h 25m 33s	12h 25m 33s
Dec	+80 11' 15"	+50 58' 49"	+06 11' 43"	06 11' 43"

3. Work description

For our work we have approximated isophotes to ellipses (with the task ellipse of IRAF), then we used DS9 to create the first ellipse that represented the first guess of the of the galaxy limit brightness. Before setting the program to create the other ellipses we had to mask the stars which with their brightness could disturb the isophotes determination. After that the program could calculate the other isophotes (Figure 3). Some ellipses were clearly not representative of the galaxy and we deleted them.

We had extracted some features of the ellipses: major semi-axis, internal flux, number of pixels restrained, coordinates of the centre, degree of position angle, intensity, ellipticity; there were some ellipses in the table with the same number of pixels so we deleted all of them except one trying to keep the growing of the major semi axis linear. We had to do that because those ellipses were useless being the same isophotes. Then we arranged a table in asci in order to build diagrams through the program TOPCAT.

We apply again the same procedure but now we fixed the coordinates of the centre, and we created the ellipses representing the isophotes of the galaxies, now all concentric. At this point, we rejected all the ellipses which were too different from the structure of the galaxy and we extracted a table containing all the features that we needed to construct the diagrams (major semi axis, internal flux, number of pixels restrained). Also in this case the table must be amended, erasing the ellipses with the same number of pixels and trying to keep the growing of the major semi axis linear.

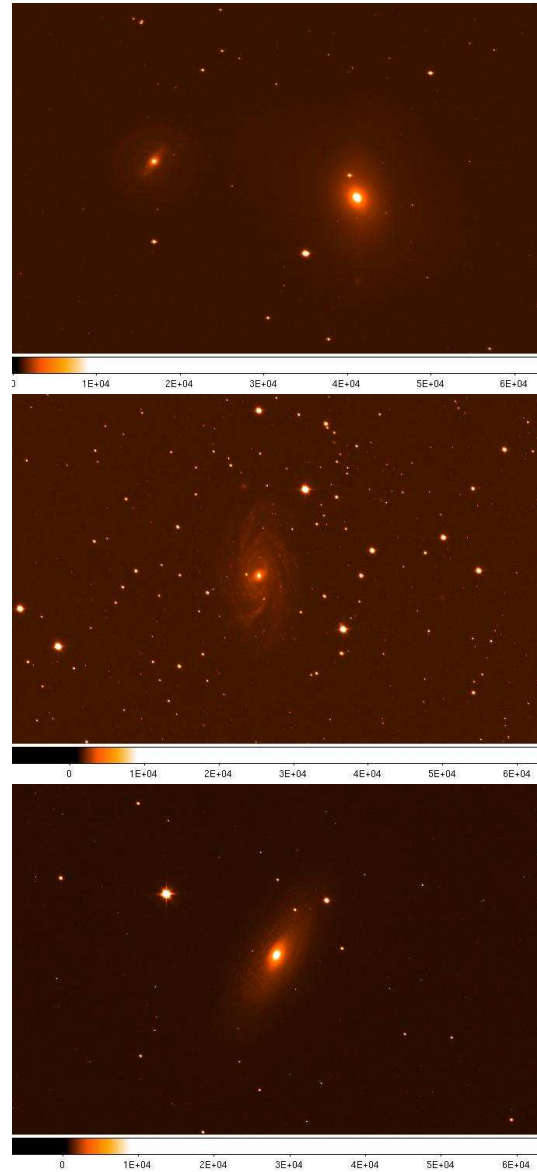


Fig. 2. Observed galaxies. *top*: NGC 4394 (*on the left*) and M85 (*on the right*), *middle*: NGC 2336, *bottom*: NGC 2841. 67/92 Schmidt Telescope + R filter, Asiago Observatory

3.1. method 1: Isophotes analysis

So the first way to analyse the morphological structure is examining the isophotes with unfixed centre of our galaxies. With TOPCAT we created some graphics, that gave us a first identification of the morphological structure of the galaxies. For each galaxy we plotted the ellipticity, polar angle and the coordinates of the center (x,y) vs the semi-major axis (Figure 4).

If ellipticity, position angle and coordinates are constant for every semi-major axis probably the galaxy will be elliptical. If there are variations, they suggest the presence of some structures: the galaxy will probably

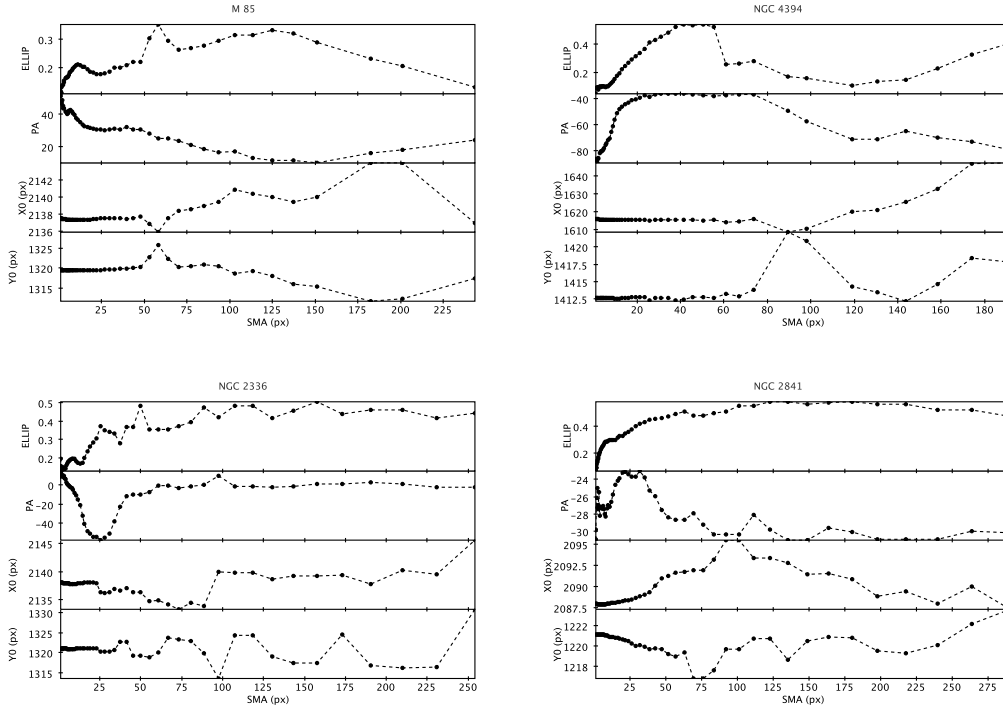


Fig. 4. For each galaxy and from the top are shown the isophote parameters, ellipticity, polar angle (*degree*), x center (*pixels*), y center (*pixels*) as function of ellipse semi-major axes (SMA, *pixels*).

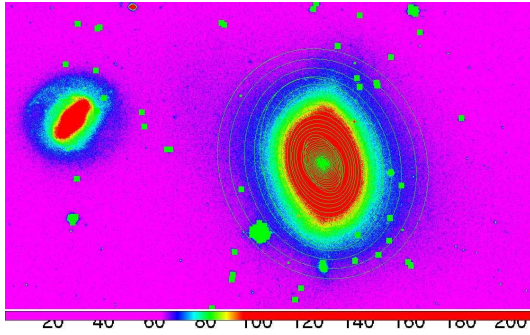


Fig. 3. The isophotes approximated by ellipses (in *green*) are overlaped to M85 (the galaxy on the right), the ellipses were determined using IRAF's task ELLIPSE, the squares and clusters of squares (in *green*) are the masked stars (see text).

be spiral. In particular, if for lower semi-major axis ellipticity changes while the position angle remains constant, we can deduce the presence of a bar.

3.2. method 2: Residuals analysis

Using the IRAF task bmodel on the isophotes with unfixed centre we created an image which approximates the galaxy. Then we subtracted the image pixel per pixel of this model from the original one of the galaxy and

we obtained a third image of the residue (Figures 5 and 6). Isophotes approximation is regular and so will be the model: any irregular structure will remain in the residue. If in this images we can notice these structures, such as bars or spiral arms, the galaxy will be spiral; if there aren't it will be elliptical.

3.3. method 3: Brightness profile

A third way to analyse the morphological structure of our galaxies is the construction of their brightness profile. Now we have to calculate some new parameters from the table of the isophotes with fixed centre, using the program TOPCAT. The semi-major axes in kpc, the sky corrected flux and the ellipse area in arcsec^2 . The flux (in counts $\text{s}^{-1} \text{arcsec}^{-2}$) between two adjacent ellipses is obtained by

$$I = (flux_2 - flux_1)/(area_2 - area_1) \quad (1)$$

the subscript 2 and 1 refer respectively to the adjacent ellipses. Then the observed calibrated brightness is obtained

$$I_{sup} = (I < I_{sky} > N_{pix})/(t_{exp} A) \quad (2)$$

where $< I_{sky} >$ is the sky mean intensity, N_{pix} the number of pixel between two ellipses, t_{exp} the exposure time and A the pixel area in arcsec .

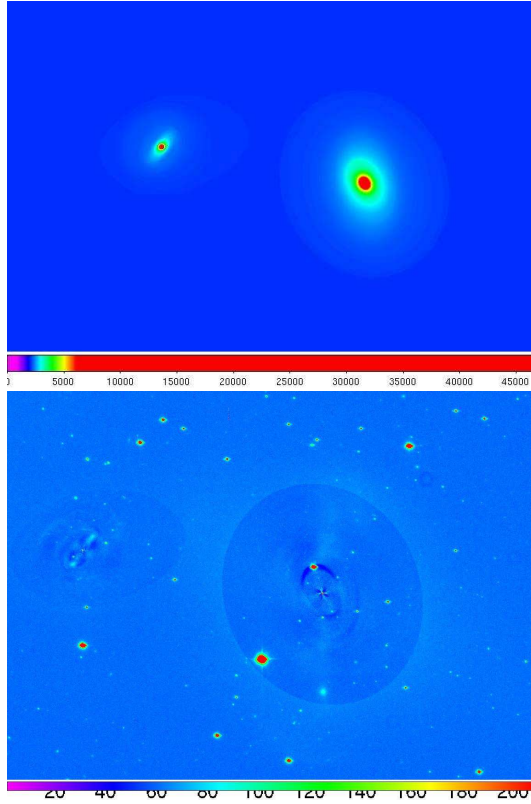


Fig. 5. The figures show respectively the models (top) and residuals (bottom) of NGC 4294 and M85. The models were created assuming the isophotes, approximated by ellipses, as the real brightness distribution of the galaxies. Residual image is found through the subtraction between the original image and the model.

Now it is possible to determine the instrumental surface brightness by the classical relation between intensity and magnitude (Karttunen et al. , 1996)

$$\mu = -2.5 \text{Log } I_{sup} \quad (3)$$

Finally this value must be calibrated taken into account the atmospheric extinction ($k x$, where k is the extinction coefficient and x the airmass) and the zero point of scale magnitude (m_0)

$$m_{cal}^{obs} = \mu + m_0 + k x \quad (4)$$

In our case $m_0 + k x \approx 5$ and we adopted this value as calibration coefficient.

Now we can construct the brightness profile graphics, placing on the abscissa the semi-major axis and on the ordinate the observed calibrated brightness. At this point we have to study the brightness profile of every galaxy using two different rules. We can approximate the bulge using the De Vaucouleurs law (Simien & de Vaucouleurs , 1986), (Equation 5) while for the disk we can use the exponential disk law

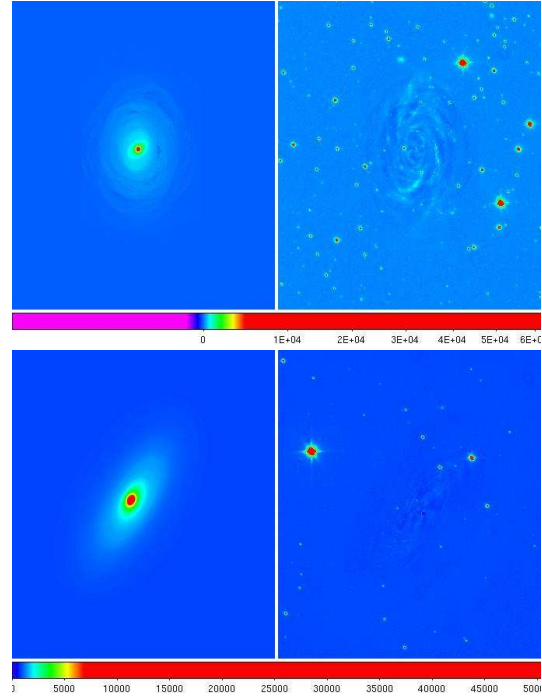


Fig. 6. The figures show respectively the models (on the left) and residuals (on the right) of NGC 2336 and NGC 2841.

Table 3. Bulge and disk coefficients

Object	μ_e	r_e	μ_0	h
NGC 2336	26.0	35	23.8	45
NGC 2841	24.0	40	23.2	75
M85	23.7	35	23.5	65
NGC 4394	24.4	20	23.5	30

(Equation 6). For an elliptical galaxy we can approximate the entire galaxy with the first law, but for a spiral galaxy we have to add to it the second model.

$$\mu_{bulge} = \mu_e 8.325 ((r/r_e)^{1/4} - 1) \quad (5)$$

$$\mu_{disk} = \mu_0 1.085 (r/h) \quad (6)$$

where r_e is the distance from the centre in which we find half of the light of the bulge, μ_e is the magnitude respective to r_e , μ_0 is the magnitude in the center and h represents the distance in which

$$I = I_0/e \quad (7)$$

The parameters were found empirically in order to reproduce the brightness profiles (Figures 7) the values are reported in Table 3. Then by Equation 3, the brightness of each component was found (Table 4).

The total intensity of bulge and disk were calculated by means the following equations

$$I_{bulge}^{tot} = 11.93 I_e r_e^2 = B \quad (8)$$

Table 4. Bulge and disk intensities

Object	I_e	B	I_0	D
NGC 2336	$2.5 \cdot 10^{-11}$	$3.7 \cdot 10^{-7}$	$3.0 \cdot 10^{-10}$	$4.0 \cdot 10^{-6}$
NGC 2841	$2.5 \cdot 10^{-10}$	$4.8 \cdot 10^{-6}$	$5.0 \cdot 10^{-10}$	$1.8 \cdot 10^{-5}$
M 85	$3.3 \cdot 10^{-10}$	$4.8 \cdot 10^{-6}$	$4.0 \cdot 10^{-10}$	$1.1 \cdot 10^{-5}$
NGC 4394	$1.7 \cdot 10^{-10}$	$8.1 \cdot 10^{-7}$	$4.0 \cdot 10^{-10}$	$2.3 \cdot 10^{-6}$

$$I_{disk}^{tot} = 2\pi I_0 h^2 = D \quad (9)$$

Now we can find the morphological type using the T-Type scale (Simien & de Vaucouleurs, 1986). From the ratio $B/(B+D)$ we find Δm using

$$\Delta m = -2.5 \text{Log}[B/(B+D)] \quad (10)$$

With Δm it is possible to obtain the parameter T (Table 5) exploiting the graphic reported in Simien & de Vaucouleurs (1986).

Table 5. T-Type classification

Object	$B/(B+D)$	Δm	T
NGC 2336	0.08	2.74	~ 5
NGC 2841	0.21	1.69	~ 3
M 85	0.31	1.27	~ 1.5
NGC 4394	0.26	1.46	~ 3

4. Results

In this work we classified the morphological type of four galaxies, NGC 2336, NGC 2841, M 85 and NGC 4394, through three different methods, a) isophote analysis, b) residual analysis, c) brightness profile. The isophotes, approximated by ellipses, were determined in two ways, respectively with free and fixed centers. The ellipses with free centers were used to analyse the isophote parameters, ellipticity, polar angle and the coordinates of the center (x,y), as function of the semi-major axis, and to build the models of the galaxies in order to find the residual maps subtracting the model from the original image. Ellipses with fixed center were used in order to find the brightness profile and to fit it through a composition of two models, respectively for the bulge and disk components. Concerning the first method we can deduce only an approximate classification, if the galaxy is an elliptical or a spiral, maybe with a bar. With the residuals method peculiar structures become more clear, of course the results depend on the goodness of the model. Finally from the brightness profile analysis it is not possible to throw up bars or other peculiar structures because we analyse the mean brightness between two adjacent ellipses and the models we built are based on two regular components, respectively bulge and disk.

With the first method we found well defined trends, increasing or decreasing values with the semi-major axis, and sometime large variations, in both ellipticity and polar angle up to 40 arcsec from the center, in NGC

2841 the variations affect the center coordinates too. In the case of M85 we found a variation of the center coordinates and ellipticity between 50 and 60 arcsec where the polar angle shows a regular trend, this could be due to a not corrected determination of the ellipsis, if we remove these points the trends are regular for all the parameters excluding the inner parts of the galaxy (< 10 arcsec) where a variation in polar angle and ellipticity is however seen. Ultimately M 85 is S type with a possibility of inner substructures. Otherwise the presence of substructures is clear in the other three objects, so we can conclude that the morphological type is S. The residual images show substructures indicative of spiral arms in all the objects except M85, in this case the residuals show a cross shape feature, typical of elliptical galaxies, although it appears weakly distorted like spiral arms, so the morphological type could be classified as intermediate between E and S but the presence of a disk is undoubted. Furthermore, the residuals of NGC 2336 and NGC 4294 show a clear evidence of bars. Finally, from the brightness profile we confirmed the S type for all the galaxies.

At the end we compared our results with the official data (SIMBAD). The results are summarized in the Table 6. Concerning NGC 2336, NGC 2841 and NGC 4394, our findings are in accord with the published morphological types, these classifications are used recently by many authors (i.e. Wilke K., Möllenhoff C., & Matthias M. (1999) for NGC 2336, Blais-Ouellette S. et al. (2004) for NGC 2841 and Vicari, A. et al. (2002) for NGC 4394. M85 is classified like S0, with the third method we obtained an higher morphological type, Sa, the disk component appears overestimated, this could be due to an incorrect model used in the fitting, we applied only the De Vaucouleurs law. The presence of possible substructures in the inner part of the galaxy pointed out with the first method could be real, because this galaxy is a product of a recent merge (Lauer et al. , 2005).

Table 6. Classification

Object	method 1	2	3	SIMBAD
NGC 2336	S	SB	Sc	SBc
NGC 2841	S	S	Sb	Sb
M 85	S	E/S	Sa	S0
NGC 4394	S	SB	Sb	SBb

References

- Blais-Ouellette S., Amram P., Carignan C., & Swaters R. 2004, A&A, 420, 147B
Karttunen, H., Kröger, P., Oja, H., Poutanen, M., & Donner, K. J. 1996, Fundamental Astronomy, Springer-Verlag Berlin Heidelberg New York
Lauer T. R. et al. 2005, AJ, 129, 2138L
Simien, de Vaucouleurs 1986, ApJ, 302, 574-578

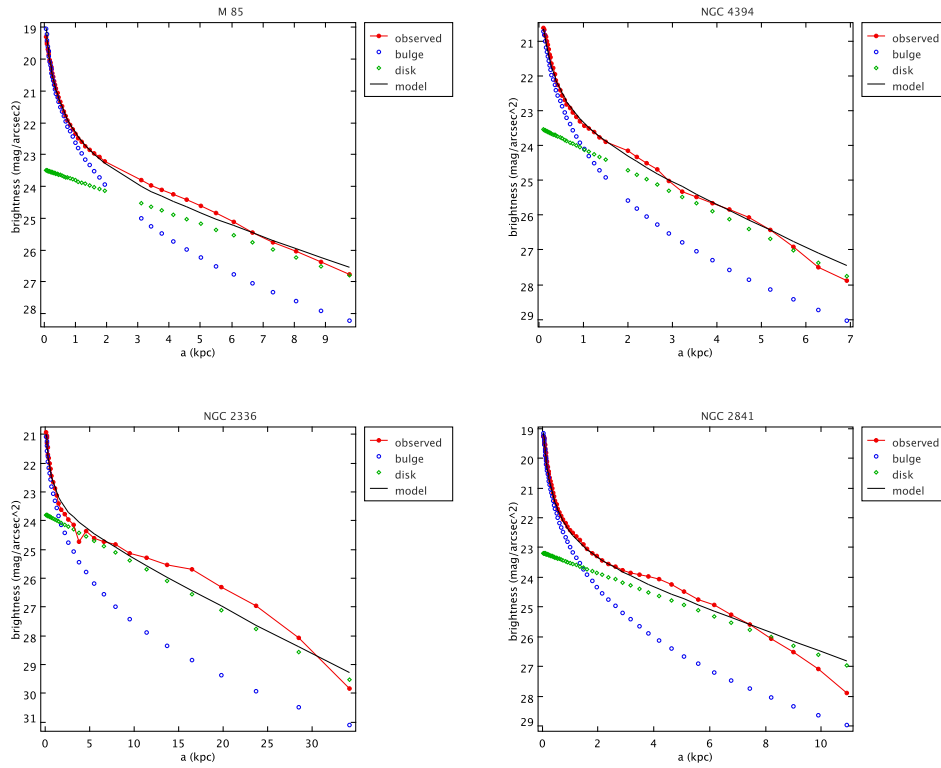


Fig. 7. For each galaxy are indicated respectively the brightness profile, $\text{mag}/\text{arcsec}^2$ (*red dots and continuous line*), the isophotes were approximated by ellipses with fixed center), the bulge (*blue circles*) and disk (*green diamonds*) model profiles and the composition of both models (*black continuous line*) versus the semi-major axes, kpc.

Vicari A., Battinelli P., Capuzzo-Dolcetta R., Wyder
 T. K., & Arrabito, G. 2002, *A&A*, 384, 24
 Wilke K., Möllenhoff C. & Matthias, M. 1999, *A&A*,
 344, 787
 SIMBAD, <http://simbad.u-strasbg.fr/simbad/>
 wikipedia, <http://en.wikipedia.org/wiki>